

# Numerical Simulations of $\mathcal{PT}$ -Symmetric Quantum Field Theories

Claude Bernard\* and Van M. Savage†

*Department of Physics, Washington University, St. Louis, Missouri 63130, USA*

(July 23, 2021)

## Abstract

Many non-Hermitian but  $\mathcal{PT}$ -symmetric theories are known to have a real positive spectrum. Since the action is complex for these theories, Monte Carlo methods do not apply. In this paper the first field-theoretic method for numerical simulations of  $\mathcal{PT}$ -symmetric Hamiltonians is presented. The method is the complex Langevin equation, which has been used previously to study complex Hamiltonians in statistical physics and in Minkowski space. We compute the equal-time one-point and two-point Green's functions in zero and one dimension, where comparisons to known results can be made. The method should also be applicable in four-dimensional space-time. Our approach may also give insight into how to formulate a probabilistic interpretation of  $\mathcal{PT}$ -symmetric theories.

Typeset using REVTeX

---

\*electronic mail: [cb@lump.wustl.edu](mailto:cb@lump.wustl.edu)

†electronic mail: [vmsavage@hbar.wustl.edu](mailto:vmsavage@hbar.wustl.edu)

## I. INTRODUCTION

Traditionally, only theories with Hermitian Hamiltonians are studied in quantum mechanics and quantum field theory. This is because Hermiticity guarantee real eigenvalues and therefore unitary time translation and conservation of probability. It has recently been observed that quantum mechanical theories whose Hamiltonians are not Hermitian but are symmetric under a transformation known as  $\mathcal{PT}$  symmetry have positive definite spectra [1–16]. A major criticism of these theories is that a consistent probabilistic interpretation has not been formulated. This paper suggests that there is a real, Fokker-Planck probability underlying these theories and presents a numerical method for calculating the  $k$ -point Green's functions,  $G_k$ , of these theories.

A  $\mathcal{PT}$ -symmetric Lagrangian that has been studied in the past is defined by the Euclidean Lagrangian

$$\mathcal{L}_E = \frac{1}{2}(\partial\phi)^2 + \frac{1}{2}m^2\phi^2 - \frac{g}{N}(i\phi)^N. \quad (1.1)$$

A recent paper used Schwinger-Dyson techniques to study this self-interacting scalar quantum field theory [17]. Green's functions,  $G_k$ , calculated by this method agreed extremely well with known results. It was argued that these theories possess a positive definite spectrum and a nonvanishing value of  $G_1 = \langle 0|\phi|0\rangle$  for all  $N > 2$ .

Under  $\mathcal{PT}$  symmetry  $\mathcal{P}$  sends  $\phi \rightarrow -\phi$  and  $\mathcal{T}$  sends  $t \rightarrow -t$  and  $i \rightarrow -i$ , where  $t$  is time. (Note that in one dimension (i.e. quantum mechanics)  $\phi$  represents the position of the particle and  $\mathcal{P}$  corresponds to reflection in space.) Thus,  $\mathcal{L}_E$  is manifestly  $\mathcal{PT}$  symmetric. It is believed that the reality and positivity of the spectra are a direct consequence of this  $\mathcal{PT}$  symmetry. The positivity of the spectra for all  $N$  is an extremely surprising result; it is not at all obvious, for example, that the Lagrangian  $\mathcal{L}_E = (\partial\phi)^2/2 - g\phi^4/4$  corresponding to  $N = 4$  and  $m = 0$  has a positive spectrum. To understand this and other results, we must properly define the contours of integration for path integrals and, in dimension  $D > 0$ , the boundary conditions in the corresponding Schrödinger equation.

Contours of integration and boundary conditions have been extensively studied in zero and one dimension [1,17]. In zero dimensions one must choose the contour of integration for the path integral such that it lies in a region where  $\exp(-S(\phi))$  is damped as  $|\phi| \rightarrow \pm\infty$  and the path integral converges. For massless versions of Eq. (1.1), these regions are wedges and are chosen to be analytic continuations of the wedges for the harmonic oscillator, which are centered about the negative and positive real axes and have angular opening  $\frac{\pi}{2}$ . For arbitrary  $N > 2$  the anti-Stokes' lines at the centers of the left and right wedges lie below the real axis at the angles

$$\begin{aligned}\theta_{\text{left}} &= -\pi + \left(\frac{(N-2)\pi}{2N}\right), \\ \theta_{\text{right}} &= -\left(\frac{(N-2)\pi}{2N}\right).\end{aligned}\tag{1.2}$$

The opening angle of these wedges is  $\frac{\pi}{2N}$ .

Similarly, for one-dimensional versions of Eq. (1.1) with  $m = 0$ , the Schrödinger differential equation is

$$-\psi''(\phi) - \frac{g(i\phi)^N}{N}\psi(\phi) = E\psi(\phi).\tag{1.3}$$

In Ref. [1] it was shown how to continue analytically in the parameter  $N$  away from the harmonic oscillator value  $N = 2$ . This analytic continuation defines the boundary conditions in the complex- $\phi$  plane. The regions in the cut complex- $\phi$  plane in which  $\psi(\phi)$  vanishes exponentially as  $|\phi| \rightarrow \infty$  are once again wedges. These wedges also define the regions in which  $\exp(-S(\phi))$  is exponentially damped and the corresponding path integrals are convergent in one dimension. Once again, the wedges for  $N > 2$  were chosen to be analytic continuations of the wedges for the harmonic oscillator. For arbitrary  $N > 2$  the anti-Stokes' lines at the centers of the left and right wedges lie below the real axis at the angles

$$\begin{aligned}\theta_{\text{left}} &= -\pi + \left(\frac{N-2}{N+2}\right)\frac{\pi}{2}, \\ \theta_{\text{right}} &= -\left(\frac{N-2}{N+2}\right)\frac{\pi}{2}.\end{aligned}\tag{1.4}$$

The opening angle of these wedges is  $\frac{2\pi}{N+2}$ .

Consequently, expectation values for  $\mathcal{PT}$ -symmetric theories can be understood as path integrals that have been analytically continued in  $N$ . This analytic continuation deforms the contour from the real axis for the harmonic oscillator,  $N = 2$ , to contours in the complex- $\phi$  whose endpoints lie in wedges where  $\exp(-S(\phi))$  is damped as  $|\phi| \rightarrow \infty$  and the path integral converges. Defining the complex variable  $\phi_C$  to follow any contour whose endpoints lie in the appropriate wedges,  $\mathcal{PT}$ -symmetric expectation values of operators  $A = A(\phi)$  are given by:

$$\frac{\langle 0|A|0\rangle}{\langle 0|0\rangle} = \frac{\int D\phi_C A(\phi_C) e^{-S(\phi_C)}}{\int D\phi_C e^{-S(\phi_C)}}, \quad (1.5)$$

where  $S(\phi_C) = \int d^D X \mathcal{L}_E[\phi_C(X)] = \int d^D X H[\phi_C(X)]$  is the Euclidean space action. The most common choice of contour is the one along which  $\exp(-S(\phi))$  is purely damped. This contour is defined as  $\phi_C = r \exp(i\theta_L)$ ,  $-\infty \leq r \leq 0$  and  $\phi_C = r \exp(i\theta_R)$ ,  $0 \leq r \leq \infty$ , where  $\theta_L$  and  $\theta_R$  are defined by Eq. (1.2) or Eq.(1.4).

As mentioned, another remarkable property of the Lagrangian in Eq. (1.1) is that for all  $N > 2$  the expectation value  $G_1 = \langle 0|\phi|0\rangle$  of the position operator  $\phi$  in the ground state is nonzero. This surprising result shows that the theory is not parity symmetric even when  $N$  is even. The violation of parity symmetry is a consequence of the manner in which the boundary conditions and path integral contours are defined. The boundary conditions require that as  $|\phi| \rightarrow \infty$  the anti-Stokes' lines are in the lower half of the complex- $\phi$  plane for  $N > 2$ . While Eq. (1.1) appears to be invariant under a parity transformation, the anti-Stokes' lines are sent to the upper half of the complex- $\phi$  plane; this corresponds to a different set of boundary conditions. Thus, the theory is not parity symmetric except for the special case of  $N = 2$  where the anti-Stokes' lines are the real axis. Notice that if we now perform a time reversal transformation, complex conjugation sends the anti-Stokes' lines back down into the complex- $\phi$  plane, and both Eq. (1.1) and the boundary conditions are identical to the original formulation of the theory. That is, these theories are  $\mathcal{PT}$ -symmetric, but they are not symmetric under  $\mathcal{P}$  or  $\mathcal{T}$  separately. As a result,  $G_1$  is pure imaginary and  $G_2$  is real.

The results for  $\mathcal{PT}$ -symmetric but non-Hermitian theories suggest that these completely new theories may describe physical processes. Previous studies have obtained extensive results in zero and one dimension (i.e. quantum mechanics) but have been unable to perform calculations in higher dimensions. Here, we use the complex Langevin method to calculate the equal-time one-point and two-point Green's functions for massless versions of Eq. (1.1) in zero and one dimension with  $N = 3$  and  $N = 4$ . The results are in good agreements with those computed by numerical integration [1] and by variational methods [14,17]. Reference [18] studies complex Hamiltonians using the Langevin approach in higher dimensions and also obtains accurate results. This suggests that the complex Langevin method is the robust numerical method needed for studying  $\mathcal{PT}$ -symmetric theories in higher dimensions. Consequently, we are currently performing field-theoretic, numerical simulations for  $\mathcal{PT}$ -symmetric Hamiltonians in two space-time dimensions. The current paper also reveals an underlying real Fokker-Planck probability for these theories. We believe our results represent a significant step towards a physical understanding of  $\mathcal{PT}$ -symmetric theories.

This paper is organized as follows: In Sec. II we explain why Monte Carlo techniques cannot be used for these theories and review the Langevin equation as a numerical procedure for quantum field theories. In Sec. III we review the complex Langevin method and use the methods of supersymmetric quantum mechanics to derive the conditions that guarantee convergence for the expectation values. First and second-order algorithms for implementing the Langevin method are presented in Sec. IV, and the results of numerical simulations are given and shown to be in excellent agreement with known results. Sec. V contains concluding remarks concerning the implications of this study in regard to probability and completeness and proposes higher-dimensional  $\mathcal{PT}$ -symmetric theories to which this numerical method could be applied.

## II. THE LANGEVIN METHOD

Since many  $\mathcal{PT}$ -symmetric theories possess a real positive spectrum and a nonvanishing value for  $G_1$ , it has been speculated that  $\mathcal{PT}$ -symmetric theories could be used to describe a Higgs Boson. A  $-g\phi^4/4$  theory is especially interesting as a theory for the Higgs because it has a dimensionless coupling constant and is asymptotically free [17]. However, the Schwinger-Dyson equations mentioned in Sec. I are too difficult to solve in four-dimensional space-time, where physical quantities must be calculated. Hence, a reliable numerical method is needed to compute expectation values in higher dimensions. In this section we argue that Monte Carlo methods are ill suited for these theories, while the complex Langevin equation provides a robust numerical technique.

Most often, Monte Carlo methods are used for numerical evaluations of expectation values like those in Eq. (1.5) where the contour of integration is along the real axis and  $S(\phi)$  is real. This is achieved by choosing paths weighted according to the probability distribution,  $\exp(-S(\phi))$ . For the Hamiltonians considered in this paper,  $S(\phi)$  is complex, and neither a real representation nor a consistent probabilistic interpretation is known. One approach to use Monte Carlo is to separate the Hamiltonian into real and imaginary parts and consider  $A(\phi) \exp(-i\text{Im}[S(\phi)])$  the operator and  $\exp(-\text{Re}[S(\phi)])$  the probability distribution. There are two problems with this approach. Firstly, the size of  $\text{Im}[S(\phi)]$  increases with the size of the lattice, making the numerator and denominator of Eq. (1.5) very small. Consequently, numerical simulations become very difficult. Secondly, and more importantly, in many cases  $\text{Im}[S(\phi)]$  contains more information about which paths are important than  $\text{Re}[S(\phi)]$ . Therefore, the algorithm outlined above never samples the important paths and thus fails to converge to the correct answer. Specific examples of this phenomenon are given in Refs. [19–21]. Our studies of zero-dimensional versions of Eq. (1.1) suggest that this is the case for non-Hermitian but  $\mathcal{PT}$ -symmetric theories, and that Monte Carlo methods are inapplicable.

Another method for numerical calculations in quantum field theory involves the Langevin

equation [22,23],

$$\frac{\partial\phi}{\partial\tau} = -\frac{\partial S(\phi)}{\partial\phi} + \eta(\tau), \quad (2.1)$$

where  $\tau$  is an unphysical, Langevin time,  $\partial S(\phi)/\partial\phi$  gives the equations of motion for the Hamiltonian, and  $\eta(\tau)$  is a stochastic variable. The function  $\eta(\tau)$  is chosen to be a real, Gaussian random function that satisfies the conditions

$$\langle\eta(\tau)\rangle = 0, \quad \langle\eta(\tau)\eta(\tau')\rangle = 2\delta(\tau - \tau'), \quad (2.2)$$

where the averaging is performed with respect to the appropriately normalized Gaussian probability distribution. Further, it is well known that when  $S(\phi)$  is real, the probability distribution,  $P(\phi, \tau)$ , associated with Eq. (2.1) is given by the Fokker-Planck equation [22,23]

$$\frac{\partial P(\phi, \tau)}{\partial\tau} = \frac{\partial}{\partial\phi} \left( \frac{\partial}{\partial\phi} + \frac{\partial S(\phi)}{\partial\phi} \right) P(\phi, \tau). \quad (2.3)$$

The space-time dependence of all variables and the  $\tau$  dependence of  $S$  and  $\phi$  are left implicit in the above equations. These dependencies are only made explicit when relevant to a calculation.

It is easy to evolve Eq. (2.1) numerically in Langevin time,  $\tau$ , and find expectation values. For real variables these expectation values are expressible as

$$\frac{\langle 0|A|0\rangle_P}{\langle 0|0\rangle_P} = \frac{\int D\phi A(\phi)P(\phi, \tau)}{\int D\phi P(\phi, \tau)}, \quad (2.4)$$

and one can show that

$$P(\phi, \tau) \rightarrow e^{-S(\phi)}, \quad \tau \rightarrow \infty. \quad (2.5)$$

Hence,

$$\frac{\int D\phi A(\phi)P(\phi, \tau)}{\int D\phi P(\phi, \tau)} \rightarrow \frac{\int D\phi A(\phi)e^{-S(\phi)}}{\int D\phi e^{-S(\phi)}}, \quad \tau \rightarrow \infty. \quad (2.6)$$

That is, when  $S(\phi)$  and  $\phi$  are both real, the physical expectation values are recovered by taking the unphysical, Langevin time to infinity

More generally, an analytically continued version of Eq. (2.5) often holds as long as the supersymmetric Fokker-Planck Hamiltonian,  $H_{FP}$ , formed by taking  $\partial S/\partial\phi$  as the superpotential, has a spectrum with positive real part and a ground state that is nondegenerate [18,24]. When  $S(\phi)$  is complex,  $H_{FP}$  can still have a nondegenerate ground state and a spectrum that is real and positive. As explained in Sec. III, these criteria are the correct ones to test for convergence of expectation values for the Hamiltonians studied in this paper. This is also true for several other cases studied in Refs. [25–30]. This method was successful in several cases including statistical mechanics problems with complex chemical potentials, field-theoretic calculations in Minkowski space, simulations dealing with the many Fermion problem [31], and even non-Hermitian Hamiltonians with complex eigenvalues [19].

The previous studies involving the complex Langevin equation focused on cases where the physical Hamiltonians were either Hermitian, non-Hermitian with a positive real part, or non-Hermitian with a real part that was negative and an imaginary part that was small. These cases were studied because the associated Fokker-Planck Hamiltonian,  $H_{FP}$ , had eigenvalues with a positive, real part. In contrast,  $\mathcal{PT}$ -symmetric Hamiltonians such as Eq. (1.1) often have a real part that is not strictly positive and an imaginary part that cannot be considered small. However, in the cases we have studied,  $H_{FP}$  still possesses a spectrum that is purely real and positive.

Reference [32] demonstrates that the renormalized mass squared for the anharmonic oscillator,  $M_1^2 = (E_1 - E_0)^2$ , is proportional to the first nonzero eigenvalue of the associated Fokker-Planck Hamiltonian. This suggests that the positive real part of the spectrum of  $H_{FP}$  is a consequence of the purely real spectrum of these  $\mathcal{PT}$ -symmetric Hamiltonians. For the zero-dimensional  $\mathcal{PT}$ -symmetric Hamiltonians studied in this paper, the eigenvalues of the associated  $H_{FP}$  are always positive and real. We believe that a  $\mathcal{PT}$ -symmetric Hamiltonian with real, positive eigenvalues will always lead to a real positive part for the eigenvalues of  $H_{FP}$ . To prove this would be tantamount to finding the exact conditions necessary for a given  $\mathcal{PT}$ -symmetric Hamiltonian to possess a real spectrum, and that is an open problem. Moreover, in Ref. [32] and elsewhere, Hermitian Hamiltonians in Minkowski space often lead



to an associated  $H_{FP}$  that is non-Hermitian. In contrast, the  $\mathcal{PT}$ -symmetric, non-Hermitian Hamiltonians in this paper always lead to Fokker-Planck Hamiltonians that maintain  $\mathcal{PT}$  symmetry; this is explained in Sec. III.

### III. COMPLEX LANGEVIN EQUATION

To gain a deeper understanding of when the Langevin equation works and of its connection to the Hamiltonian being studied, we begin with the complex Fokker-Planck equation. Allowing  $S(\phi)$  and  $\phi$  to be complex, Eq.(2.1) can be divided into its real and imaginary parts and written as two coupled equations. If one assumes the noise is purely real and uses the standard methods of stochastic calculus to derive Ito's formula for two variables [23], one is lead to the complex Fokker-Planck equation,

$$\begin{aligned} \frac{\partial P(\phi_R, \phi_I; \tau)}{\partial \tau} &= \left( \frac{\partial}{\partial \phi_R} \text{Re} \left[ \frac{\partial S}{\partial \phi} \right] + \frac{\partial}{\partial \phi_I} \text{Im} \left[ \frac{\partial S}{\partial \phi} \right] + \frac{\partial^2}{\partial \phi_R^2} \right) P(\phi_R, \phi_I; \tau) \\ &\equiv O_{FP}(\phi_R, \phi_I) P(\phi_R, \phi_I; \tau), \end{aligned} \quad (3.1)$$

where  $\phi_R$  and  $\phi_I$  are the real and imaginary parts of  $\phi$  respectively and  $S = S(\phi_R + i\phi_I)$ . Eq.(3.1) defines a purely real probability in the complex- $\phi$  plane, but apart from a few simple cases [28,29], explicit constructions of  $P(\phi_R, \phi_I; \tau)$  are unknown.

Now that we are evolving the Langevin equation in the complex plane, Eq.(2.4) must be modified. The average over the Langevin probability must be taken as an area integral in the complex plane given by

$$\frac{\langle 0|A|0 \rangle_P}{\langle 0|0 \rangle_P} = \frac{\int D\phi_R D\phi_I A(\phi_R + i\phi_I) P(\phi_R, \phi_I; \tau)}{\int D\phi_R D\phi_I P(\phi_R, \phi_I; \tau)}. \quad (3.2)$$

Notice that  $A(\phi_R + i\phi_I)$  is an analytic function, but  $P$  is not in general. Understanding how Eq.(2.5) and Eq.(2.6) are satisfied is now much more complicated because in the limit  $\tau \rightarrow \infty$  one must show how an area integral becomes a path integral and that a real, nonanalytic function,  $P$ , generates the complex, analytic function  $\exp(-S(\phi))$ . This can be achieved in a formal manner by following the approach introduced in Refs. [25,27].

For the case of  $ig\phi^3/3$  in zero dimensions with  $m = 0$ , the path integral converges when  $\exp(-S(\phi))$  is exponentially damped. Expressing the complex variable in polar coordinates,  $\phi = r \exp(i\theta)$ , the Stokes' regions that are traditionally chosen for  $\mathcal{PT}$ -symmetric theories are  $-\pi < \theta < -2\pi/3$  and  $-\pi/3 < \theta < 0$ , as discussed in Sec. I. These wedges are depicted in Fig. 1. Moreover, analytical calculations for these theories are most easily done along the contour where there is pure exponential damping defined by  $\theta = -5\pi/6$  and  $\theta = -\pi/6$ . This contour is the dashed line in Fig. 1. However, any contour whose endpoints lie in the appropriate Stokes wedges is acceptable. For purposes of proving convergence for the Langevin expectation values, the easiest contour to use is  $\phi = \phi_R - ib$ , where  $b$  is any finite constant. Along this contour,  $\exp(-S(\phi)) = \exp(-ig\phi^3/3) \sim (\text{oscillatory term}) * \exp(-g\phi_R^2 b)$ , and is therefore damped as  $\phi_R \rightarrow \pm\infty$ . This contour is the solid line in Fig. 1.

The large  $\tau$  behavior of the expectation values given by Eq.(3.2) is discovered by shifting integration variables,  $\phi_I \rightarrow \phi_I - b$ . This shift does not affect the endpoints of integration and has a Jacobian of one. Any analytic function  $A(\phi_R - ib + i\phi_I)$  can be Taylor expanded about the contour,  $\phi_C = \phi_R - ib$ . This allows us to express the expectation values as

$$\frac{\langle 0|A|0\rangle_P}{\langle 0|0\rangle_P} = \frac{\int D\phi_R D\phi_I \left( e^{i\chi} A(\phi_C) \right) P(\phi_R, \phi_I - b; \tau)}{\int D\phi_R D\phi_I P(\phi_R, \phi_I - b; \tau)}, \quad (3.3)$$

where

$$\chi = \phi_I \frac{\partial}{\partial \phi_R}. \quad (3.4)$$

Integrating Eq.(3.3) by parts infinitely many times gives:

$$\frac{\langle 0|A|0\rangle_P}{\langle 0|0\rangle_P} = \frac{\int D\phi_R A(\phi_C) P_{eff}(\phi_C, \tau)}{\int D\phi_R P_{eff}(\phi_C, \tau)}, \quad (3.5)$$

where

$$P_{eff}(\phi_C, \tau) = \int D\phi_I e^{-i\chi} P(\phi_R, \phi_I - b; \tau). \quad (3.6)$$

We assume that  $P$  vanishes at infinity rapidly enough so that all of the boundary terms from the integration by parts are zero. (In the denominator of Eq.(3.3)  $\exp(-i\chi)$  can be

introduced for free because all but the zeroth order term in  $\chi$  integrate to zero.) Note that  $P_{eff}$  is an analytic function of  $\phi_C = \phi_R - ib$ , not a function of  $\phi_R$  and  $b$  separately. We see this by using  $\exp(-i\chi)P(\phi_R, \phi_I - b; \tau) = P(\phi_R - i\phi_I, \phi_I - b; \tau)$  and then shifting the integration variable  $\phi_I \rightarrow \phi_I + b$ , so that  $P_{eff} = \int D\phi_I P(\phi_C - i\phi_I, \phi_I; \tau)$ . As a result, Eq.(3.5) can be equivalently written as

$$\frac{\langle 0|A|0\rangle_P}{\langle 0|0\rangle_P} = \frac{\int_{-\infty-ib}^{\infty-ib} D\phi_C A(\phi_C)P_{eff}(\phi_C, \tau)}{\int_{-\infty-ib}^{\infty-ib} D\phi_C P_{eff}(\phi_C, \tau)}. \quad (3.7)$$

We now derive a pseudo Fokker-Planck equation for  $P_{eff}(\phi_C, \tau)$ . From Eqs. (3.6) and (3.1),

$$\begin{aligned} \frac{\partial P_{eff}(\phi_C, \tau)}{\partial \tau} &= \int D\phi_I e^{-i\chi} \frac{\partial P(\phi_R, \phi_I - b; \tau)}{\partial \tau} \\ &= \int D\phi_I O_{FP}^{eff} e^{-i\chi} P(\phi_R, \phi_I - b; \tau), \end{aligned} \quad (3.8)$$

where  $O_{FP}^{eff} \equiv \exp(-i\chi)O_{FP}(\phi_R, \phi_I - b)\exp(i\chi)$ . Using the relations

$$\begin{aligned} e^{-i\chi} \frac{\partial}{\partial \phi_R} e^{i\chi} &= \frac{\partial}{\partial \phi_R} \\ e^{-i\chi} \frac{\partial}{\partial \phi_I} e^{i\chi} &= \frac{\partial}{\partial \phi_I} + i \frac{\partial}{\partial \phi_R} \\ e^{-i\chi} F(\phi_C + i\phi_I) e^{i\chi} &= F(\phi_C), \end{aligned} \quad (3.9)$$

it is straightforward to show that

$$O_{FP}^{eff} = \frac{\partial}{\partial \phi_R} \left( \frac{\partial}{\partial \phi_R} + \frac{\partial S(\phi_R - ib)}{\partial \phi_R} \right) + \frac{\partial}{\partial \phi_I} e^{-i\chi} \text{Im} \left[ \frac{\partial S(\phi_R - ib + i\phi_I)}{\partial \phi} \right] e^{i\chi}. \quad (3.10)$$

The last term of Eq. (3.10) is a total derivative in  $\phi_I$ , and therefore, disappears from the right side of Eq. (3.8), again assuming  $P$  vanishes rapidly at infinity. Since the remaining terms of  $O_{FP}^{eff}$  do not depend on  $\phi_I$ , they can be pulled out in front of the integral over  $D\phi_I$ . Using the fact that  $\partial/\partial \phi_R = \partial/\partial \phi_C$  on an analytic function of  $\phi_C$ , Eq.(3.8) becomes Eq. (2.3) with  $\phi = \phi_C$  and  $P(\phi, \tau) = P_{eff}(\phi_C, \tau)$

$$\frac{\partial P_{eff}(\phi_C, \tau)}{\partial \tau} = \frac{\partial}{\partial \phi_C} \left( \frac{\partial}{\partial \phi_C} + \frac{\partial S(\phi_C)}{\partial \phi_C} \right) P_{eff}(\phi_C, \tau). \quad (3.11)$$

That is, there is a pseudo-Fokker-Planck equation that defines a complex analytic function,  $P_{eff}$ , that is just the analytic continuation of the Fokker-Planck equation for real variables.

For cases where  $N > 3$  in Eq.(1.1), a similar derivation gives the same result. The only subtlety is in choosing the correct contour. For any  $N$  a contour with finite endpoints,  $(-b, -b \cot \theta_L)$  and  $(-b, b \cot \theta_R)$ , as defined by Eq.( 1.2), can be deformed into the contour  $\phi_C = \phi_R - ib$  as shown in Fig. 2. Consequently, using the methods above, an area integral over the strip  $-b \cot \theta_L \leq \phi_R \leq b \cot \theta_R; -\infty \leq \phi_I \leq \infty$  is expressible as a path integral over the contour  $\phi_C = \phi_R - ib$  plus boundary terms involving derivatives of  $P$ . As  $b$  grows larger, the area integral approaches an integral over the entire complex plane. We expect the boundary terms to approach zero because the probability of finding a particle at  $\pm\infty$  should go to zero. This is seen in Fig. 3 (Sec. IV). Following the derivation for  $ig\phi^3/3$ , we are again led to Eq.(3.11)

Thus, the problem of understanding the  $\tau \rightarrow \infty$  behavior of expectation values has been reduced to one that is formally identical to that for real variables. We now use the methods of Parisi and Sourlas [33] who first discovered the hidden supersymmetry in classical stochastic equations.

If we express Eq.(3.11) in terms of  $p(\phi_C, \tau) \equiv P_{eff}(\phi_C, \tau) \exp(S(\phi)/2)$ , we obtain the Schrödinger equation

$$\frac{-\partial p(\phi_C, \tau)}{\partial \tau} = H_{FP} p(\phi_C, \tau) \equiv \left( -\frac{\partial}{\partial \phi_C} + \frac{1}{2} \frac{\partial S}{\partial \phi_C} \right) \left( \frac{\partial}{\partial \phi_C} + \frac{1}{2} \frac{\partial S}{\partial \phi_C} \right) p(\phi_C, \tau). \quad (3.12)$$

As claimed,  $H_{FP}$  is the supersymmetric Hamiltonian formed from the superpotential  $\partial S/\partial \phi_C$ . Since  $S$  is  $\mathcal{PT}$  symmetric,  $\partial S/\partial \phi_C$  is anti- $\mathcal{PT}$  symmetric, and  $H_{FP}$  is  $\mathcal{PT}$ -symmetric, as claimed in the last section [34]. Expanding Eq. (3.12) yields

$$H_{FP} = -\frac{\partial^2}{\partial \phi_C^2} - \frac{1}{2} \frac{\partial^2 S}{\partial \phi_C^2} + \frac{1}{4} \left( \frac{\partial S}{\partial \phi_C} \right)^2. \quad (3.13)$$

If the time-independent version of Eq. (3.12),

$$H_{FP} \Psi_k^{FP}(\phi_C) = \lambda_k \Psi_k^{FP}(\phi_C), \quad (3.14)$$

is well posed and the eigenfunctions  $\Psi_k^{FP}(\phi_C)$  are complete, then

$$p(\phi_C, \tau) = \sum_{k=0}^{\infty} a_k \Psi_k^{FP}(\phi_C) e^{-\lambda_k \tau}. \quad (3.15)$$

Note that  $\Psi_0^{FP}(\phi_C) \equiv \exp(-S(\phi_C)/2)$  is an eigenfunction of  $H_{FP}$  with  $\lambda_0 = 0$ . Therefore, Eq. (3.15) becomes

$$p(\phi_C, \tau) = C e^{-(1/2)S(\phi_C)} + \sum_{k=1}^{\infty} a_k \Psi_k^{FP}(\phi_C) e^{-\lambda_k \tau}. \quad (3.16)$$

Moreover, if the spectrum of  $H_{FP}$  is such that

$$Re[\lambda_k] > 0, \quad k > 0, \quad (3.17)$$

it follows that

$$p(\phi_C, \tau) \rightarrow C e^{-(1/2)S(\phi_C)}, \quad \tau \rightarrow \infty. \quad (3.18)$$

The  $\tau$  dependence of  $p(\phi_C, \tau)$  has disappeared in this limit. That implies  $dP_{eff}/d\tau = 0$  and signals that the system has reached equilibrium. Expressing  $P_{eff}(\phi_C, \tau)$  in terms of  $p(\phi_C, \tau)$  and taking the limit  $\tau \rightarrow \infty$  gives analytically continued versions of Eq. (2.5), and thus Eq. (2.6), in terms of  $P_{eff}$ . As a result, Langevin expectation values are shown to converge to the right side of Eq. (1.5) as  $\tau \rightarrow \infty$ . This result is true for our zero-dimensional  $\mathcal{PT}$ -symmetric theories as long as the ground state is nondegenerate. There is no evidence that  $\mathcal{PT}$ -symmetric theories possess a degenerate ground state, so for the purposes of this paper, we will not consider this a possibility.

Thus, if the supersymmetric Hamiltonian  $H_{FP}$  formed from the superpotential,  $\partial S/\partial\phi_C$ , has a spectrum satisfying Eq. (3.17), the Langevin method should work as a calculational procedure. Explicitly, we have shown that analytic continuations of Eq. (2.5) and Eq. (2.6) with  $P$  replaced by  $P_{eff}$ ,

$$P_{eff}(\phi_C, \tau) \rightarrow e^{-S(\phi_C)}, \quad \tau \rightarrow \infty \quad (3.19)$$

and

$$\begin{aligned} \frac{\int D\phi_R D\phi_I A(\phi_R + i\phi_I) P(\phi_R, \phi_I; \tau)}{\int D\phi_R D\phi_I P(\phi_R, \phi_I; \tau)} &= \frac{\int_{-\infty-ib}^{\infty-ib} D\phi_C A(\phi_C) P_{eff}(\phi_C, \tau)}{\int_{-\infty-ib}^{\infty-ib} D\phi_C P_{eff}(\phi_C, \tau)} \\ &\rightarrow \frac{\int_{-\infty-ib}^{\infty-ib} D\phi_C A(\phi_C) e^{-S(\phi_C)}}{\int_{-\infty-ib}^{\infty-ib} D\phi_C e^{-S(\phi_C)}}, \quad \tau \rightarrow \infty \end{aligned} \quad (3.20)$$

follow if  $H_{FP}$  has a nondegenerate ground state, wave functions that are complete, and a spectrum with positive real part.

#### IV. NUMERICAL METHODS AND RESULTS

In this section we apply the complex Langevin method to massless versions of Eq. (1.1) in zero and one dimension and calculate the same time one-point and two-point disconnected Green's functions for the cases  $N = 3$  and  $N = 4$ . We begin by proving (under certain assumptions) that Eq. (3.17) holds in zero dimensions and explaining the algorithms we have used to implement simulations. We then extend these results to their one-dimensional analogues.

##### A. Zero-Dimensional Theories

A recent paper by Dorey *et al.* [16] shows that  $\mathcal{PT}$ -symmetric Hamiltonians of the form,

$$\mathcal{H} = -(\partial\phi)^2 - (i\phi)^{2M} - \alpha(i\phi)^{M-1}, \quad (4.1)$$

where  $M$  and  $\alpha$  are real and boundary conditions have been chosen as in Sec. I, have a real positive spectrum if the conditions  $\alpha < M$  and  $M \geq 1$  are both satisfied [16]. (We have set  $l = 0$  in the Hamiltonian given by Dorey *et al.*) This proves (for  $\alpha = 0$ ,  $M = N/2$ ) that massless versions of Eq. (1.1) have a positive real spectrum.

In zero-dimensional studies of Eq. (1.1) with  $m = 0$ , Eq. (3.13) gives

$$H_{FP} = -\frac{\partial^2}{\partial\phi_C^2} - \frac{g(N-1)}{2}(i\phi_C)^{N-2} - \frac{g^2}{4}(i\phi_C)^{2(N-1)}, \quad (4.2)$$

where the contour,  $\phi_C$ , is within the Stokes' wedges explained in Sec. I and used by Dorey *et al.*. Making the change of variables  $\phi \rightarrow (2/g)^{1/N}\phi$ , Eq. (4.2) becomes Eq. (4.1) with  $\alpha = N - 1$  and  $M = N - 1$ . Thus,  $\alpha = M$ , and as explained in Ref. [16], this implies that the  $H_{FP}$  given in Eq. (4.2) has one zero eigenvalue, which we have already demonstrated,

and that all of the remaining eigenvalues are real and positive. Consequently, Eq. (3.17) holds for  $N \geq 2$ , and this implies that the complex Langevin method will work.

Further, the large  $\phi$  behavior of the wave functions for the eigenvalue problems defined by Eq. (4.2) must have the form

$$\Psi(\phi) \sim \exp \left[ \int d\phi \sqrt{-\frac{g^2}{4}(i\phi)^{2(N-1)}} \right] \sim \exp \left[ \frac{g}{2N}(i\phi)^N \right], \quad (4.3)$$

by *WKB*. Apart from a factor of two, the asymptotic form of the wave functions have exactly the same form as  $\exp(-S(\phi)) = \exp(g(i\phi)^N/N)$ . Thus, the Stokes' wedges that define regions of convergence for the path integral are exactly the same as those that demand  $\Psi(\pm\infty) = 0$ . This is equivalent to noting Eq. (1.4) with  $N \rightarrow 2(N-1)$  is identical to Eq. (1.2). That is, the wedges of convergence for the path integrals defined by  $\exp(-S(\phi))$  are preserved by the boundary conditions for the wave functions of the Fokker-Planck Hamiltonian.

The most general form of the Langevin equation is

$$\frac{\partial\phi}{\partial\tau} = F(\phi(\tau)) + \eta(\tau) \quad (4.4)$$

The simplest discretization of this is Euler's method (a first-order algorithm) and is explicitly given by

$$\phi(j+1) = \phi(j) + h(F(\phi(j)) + \eta(j)) = \phi(j) + \epsilon^2 F(\phi(j)) + \epsilon\eta'(j), \quad (4.5)$$

where  $j$  is an index for a Langevin-time step,  $h$  is the spacing in Langevin time,  $\epsilon = \sqrt{h}$ , and the  $h$  dependence of  $\eta(\tau)$  has been made explicit

$$\eta'(j) = \epsilon\eta(j), \quad \langle \eta'(j)\eta'(k) \rangle = 2\delta_{j,k}. \quad (4.6)$$

This form for  $\eta'(\tau)$  follows from the the normalization of the Gaussian probability distribution because Eq. (2.2) implies  $\eta^2(\tau) \sim \delta(0) \sim 1/h$  on a lattice. For this and the second order algorithm given below, there are numerical instabilities for large values of  $\phi$ . The worst instabilities arise when the potential is  $-g\phi^4/4$ . For  $-g\phi^4/4$ , it was necessary to restrict

the absolute magnitude of  $\phi$  in order to avoid these instabilities. A typical plot of the path followed by  $\phi$  in the complex plane is shown in Fig. 3.

One must then take  $\epsilon \rightarrow 0$ . Limiting values were obtained by fitting the data with second degree and third degree polynomials in  $\epsilon$ . These fits are similar to those seen in Fig. 4, which is for the one-dimensional case. Errors are calculated by collecting the simulation data in bins of a given size and computing the standard deviation of the means of the bins. The maximum error as a function of bin size is taken to be the error for the simulation. In Table I the numerical results obtained using Euler's method are compared with exact values given in Ref. [17]. The parts of the one-point and two-point disconnected Green's functions that are known to vanish (e.g.  $Re[G_1]$ ) have errors larger than their magnitude as  $\epsilon \rightarrow 0$ .

Euler's method is expected to converge linearly in  $\epsilon$  as  $\epsilon \rightarrow 0$ . Therefore, a more accurate second-order in  $\epsilon$  method is desirable. A second-order Runge-Kutta algorithm that led to good results in previous studies and was first developed in Ref. [35] is

$$\begin{aligned}\tilde{\phi}(j) &= \phi(j) + \epsilon^2 F(\phi(j)) + \epsilon \eta'(j) \\ \phi(j+1) &= \phi(j) + \frac{1}{2}\epsilon^2 (F(\phi(j)) + F(\tilde{\phi}(j))) + \epsilon \eta'(j).\end{aligned}\tag{4.7}$$

In our studies this method is more stable numerically than Euler's method, and therefore, allows the inclusion of more data. Limiting values were obtained by fitting the data with second degree and third degree polynomials in  $\epsilon$  with the linear term set equal to zero. (These fits are similar to those seen in Fig. 4 for the one-dimensional case.) The results obtained using this algorithm are compared with exact values and the result of Euler's method in Table I. There is good agreement.

It should be noted that for the case  $N = 4$ ,  $\phi(0)$  has to be chosen in the lower half of the complex- $\phi$  plane or else the numerical simulations are unstable. This is in accord with the *WKB* wedges needed to properly define the boundary conditions as explained in Sec. I. This restriction also holds in one dimension for the initial configuration at  $\tau = 0$ .



## B. One-Dimensional Theories

In this section we apply the complex Langevin method to massless versions of Eq. (1.1) in one dimension with  $N = 3$  and  $N = 4$ . The potentials are the same as those discussed in the last section, but now there is a second derivative in physical time,  $-\partial^2\phi(\tau, t)/\partial t^2$ , present in all of the equations, and  $\eta(\tau)$  becomes  $t$  dependent. Thus, the eigenvalue problem for  $H_{FP}$  becomes a partial differential equation. The spectra of eigenvalue problems for  $\mathcal{PT}$ -symmetric partial differential equations has not been studied, and we do not have a proof that they are real. But, following the examples of zero-dimensional theories, we assume the spectrum of  $H_{FP}$  has a positive real part. The results of our simulations support this assumption.

These one-dimensional theories are more computationally expensive because they give rise to Langevin equations that are partial differential equations. Consequently, the second-order algorithm in the last section is useful. For numerical simulations of one-dimensional theories, we have to introduce a physical time lattice and  $-\partial^2\phi(\tau, t)/\partial t^2$  becomes

$$-\frac{(\phi(j, l+1) - 2\phi(j, l) + \phi(j, l-1)))}{a^2}, \quad (4.8)$$

where  $l$  is an index for real time and  $a$  is the spacing in physical time. The algorithms used in the previous section are applicable here as well, but their form has changed slightly. The algorithms now contain Eq. (4.8) as part of  $F$  and the explicit lattice dependence of  $\eta(\tau, t)$  is such that

$$\eta'(j, l) = \sqrt{\hbar a} \eta(j, l), \quad \langle \eta'(j, l) \eta'(k, m) \rangle = 2\delta_{j,k} \delta_{l,m}. \quad (4.9)$$

Further, in these algorithms there is always an  $\epsilon^2$  associated with Eq. (4.8), and thus, the simulation is unstable unless  $\epsilon \ll a$ . However, there are no instabilities similar to those encountered for  $-g\phi^4/4$  in the zero dimensional case. For fixed values of  $a$ , we compute at various values of  $\epsilon$  and take the limit  $\epsilon \rightarrow 0$ , giving the expectation values as a function of  $a$ . A typical fit for this process is shown in Fig. 4. We then take  $a \rightarrow 0$  and obtain

the expectation values in the continuum limit. A fit used to extrapolate the value of  $-iG_1$  for the potential  $-g\phi^4/4$  is shown in Fig. 5. In Table II the numerical results for the expectation values are compared with numerically integrated quantum-mechanical values given in Ref. [14]. We have chosen  $g$  such that Eq. (1.1) corresponds with the Hamiltonians in Ref. [14]. The agreement of our results with previous work is excellent.

## V. CONCLUSIONS AND SPECULATIONS

This paper and Ref. [17] have shown that  $\mathcal{PT}$ -symmetric theories are amenable to the methods of quantum field theory. The previously-used Schwinger-Dyson method is very accurate but is difficult to apply to higher-dimensional theories. Here we show how a numerical method based on the complex Langevin equation can be used to obtain precise results. We believe that this numerical method can be applied to higher-dimensional theories and plan to use it for future calculations. This work represents an important step towards a test of the physical applicability of  $\mathcal{PT}$ -symmetric Hamiltonians.

An interesting implication of this study concerns the probability and completeness of  $\mathcal{PT}$ -symmetric theories. The argument for the success of the complex Langevin method in Sec. III crucially depends upon the eigenfunctions of  $H_{FP}$  being complete (3.15). Similarly, extremely accurate results in Ref. [13] crucially depend on the completeness of  $\mathcal{PT}$ -symmetric eigenfunctions. The possible connection between the eigenvalues of the Fokker-Planck Hamiltonians and the Hamiltonians being simulated suggests a possible connection between the eigenfunctions as well. Perhaps proving completeness for one of these sets of eigenfunctions would imply the completeness of the other set.

Perhaps the most important implication for  $\mathcal{PT}$ -symmetric theories is that there is an implicit probability distribution defined by Eq. (3.1) and seen in Fig. 3. Moreover, this study suggests that expectation values must be interpreted as area integrals of observables weighted by this real probability distribution. Previous studies of the zeros of eigenfunctions of  $\mathcal{PT}$ -symmetric theories suggest that the zeros interlace and become dense in a narrow band in the

complex- $\phi$  plane [36]. Hence, it was conjectured that completeness may have to be defined in terms of area integrals. We suspect a strong connection between the two results and speculate that a consistent probabilistic formulation of  $\mathcal{PT}$ -symmetric theories can only be achieved in terms of area integrals. A probabilistic interpretation of  $\mathcal{PT}$ -symmetric theories would be a major advance.

A recent study of the complex Langevin equation demonstrates that problems with convergence arise when expectation values are complex but the fixed points of the Langevin equation lie on the real axis, and as a result, the field spends most of its time on the real axis and away from the correct average value [31]. It was demonstrated there that this problem could be avoided by moving the fixed points into the complex plane. In the present study the expectation values are pure real or pure imaginary. The fixed point of the Langevin equation is zero, which is on the real axis, but the simulations converged without moving the fixed point into the complex plane. This seems to be because the path of the deterministic equation ( $\eta = 0$ ) is given by

$$\phi(\tau) = \frac{-i}{[(N-2)(\tau+C)]^{\frac{1}{N-2}}}, \quad (5.1)$$

where  $C$  is an arbitrary constant given by the initial condition. The field is attracted to the imaginary axis even though the fixed point is on the real axis. Thus, it appears to be crucial that the deterministic path to or between the fixed points is in the complex plane, but not that the fixed points themselves lie in the complex plane. The simulations for  $\mathcal{PT}$ -symmetric theories work in a straightforward manner; the fixed points do not need to be adjusted. We believe that the complex Langevin equation works so nicely for  $\mathcal{PT}$ -symmetric theories because these theories are inherently complex. As a result, it seems that  $\mathcal{PT}$ -symmetric theories may provide a class of toy models with new and interesting properties that are especially well suited for probing the intricacies of the complex Langevin equation.

The most exciting proposed application of these non-Hermitian theories is to Higgs theories. We believe that the numerical method presented in this paper should allow one to compute the mass of the Higgs particle in four-dimensional versions of these theories. Before

this can be done, however, renormalization must be thoroughly understood. Studies of field theories in fewer than four physical dimensions represent a simpler alternative. In particular, exact results for the scaling exponents of an  $ig\phi^3/3$  theory in two and three dimensions can be obtained by relating them to the Lee-Yang edge singularity in one and two dimensions respectively [37,38]. Evaluation of these exponents by the methods introduced here are in progress.

## TABLES

TABLE I. Numerically determined values of  $iG_1 = i\langle 0|\phi|0\rangle/\langle 0|0\rangle$  and  $-G_2 = -\langle 0|\phi^2|0\rangle/\langle 0|0\rangle$  using Euler's method and a second-order method for zero-dimensional  $ig\phi^3/3$  and  $-g\phi^4/4$  theories with  $g = 1/2$ . These limiting values were determined by fitting the simulated data to polynomials of second and third degree in  $\epsilon$ . For the second-order algorithm, the term linear in  $\epsilon$  is set to zero. Exact results are listed to four significant digits in the first column. Note that the values listed for the second-order algorithm are indeed more precise than the results using Euler's method.

$N$	$iG_1^{\text{exact}}$	$iG_1^{\text{Euler}}$	$iG_1^{\text{2ndorder}}$	$-G_2^{\text{exact}}$	$-G_2^{\text{Euler}}$	$-G_2^{\text{2ndorder}}$
3	0.9185	0.9198(14)	0.9194(7)	0	-	-
4	1.163	1.166(3)	1.164(1)	0.9560	0.9623(51)	0.9595(14)

TABLE II. Numerically determined values of  $iG_1 = i\langle 0|\phi|0\rangle/\langle 0|0\rangle$  and  $-G_2 = -\langle 0|\phi^2|0\rangle/\langle 0|0\rangle$  using Euler's method and a second-order method for one-dimensional  $-g(i\phi)^N/N$  theories with  $N = 3$  and  $N = 4$ . In order to compare our results with Lagrangians used in previous studies, we have set  $g = N/2$ . These continuum limit values were determined by fitting the simulated data to third degree polynomials in  $\epsilon$  for a given  $a$  (for the second-order algorithm, the term linear in  $\epsilon$  is set to zero), and then fitting the results of those fits with second degree polynomials in  $a^2$ . Exact results obtained by direct numerical integration of the quantum mechanical problem are listed to four significant digits in the first column. The exact value of  $-G_2$  for  $N = 4$  has never been directly calculated, so instead we list the results of the variational calculation given in Ref. [14]. Note that the values listed for the second-order algorithm are indeed more precise than the results using Euler's method.

$N$	$iG_1^{\text{exact}}$	$iG_1^{\text{Euler}}$	$iG_1^{\text{2ndorder}}$	$-G_2^{\text{var}}$	$-G_2^{\text{Euler}}$	$-G_2^{\text{2ndorder}}$
3	0.5901	0.5890(5)	0.5898(2)	0	-	-
4	0.8669	0.8654(6)	0.8670(3)	0.5182	0.5171(9)	0.5183(4)

## FIGURES

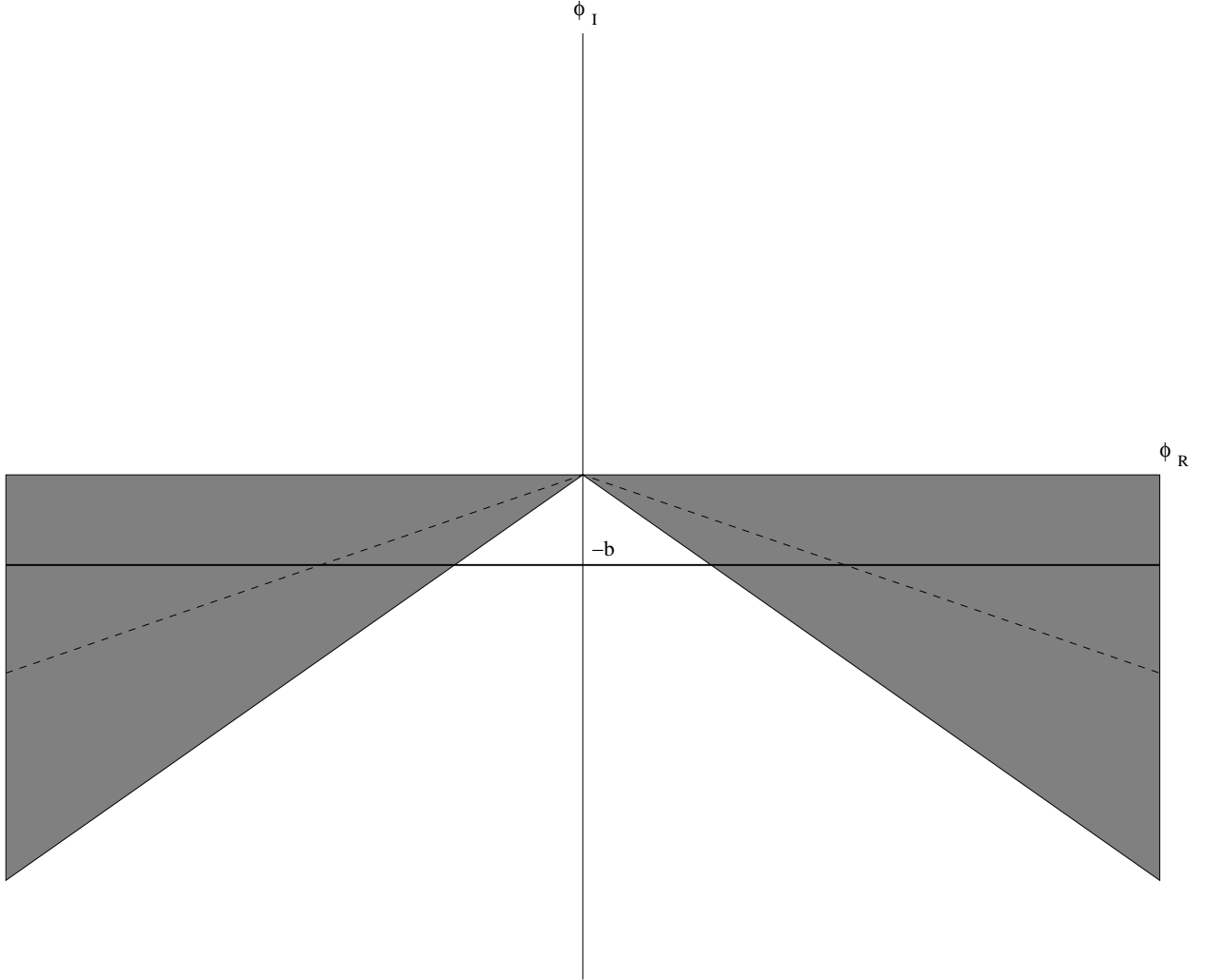


FIG. 1. Stokes' wedges for a massless, zero-dimensional  $ig\phi^3/3$  theory. The shaded areas are the regions within which the path integral for this theory converges because  $\exp(-S(\phi))$  is exponentially damped. The usual path of integration is represented by the dashed line and extends from  $-\infty$  to the origin along the ray defined by  $\theta_R = -5\pi/6$  and then from the origin to  $\infty$  along the ray defined by  $\theta_L = -\pi/6$ . Along this contour  $\exp(-S(\phi))$  is purely exponentially damped. In order to prove that the Langevin expectation values have the desired behavior as  $\tau \rightarrow \infty$ , it is easiest to use the smooth contour represented by the solid line. The solid line contour is defined as  $\phi = \phi_R - ib$  and extends from  $-\infty - ib \rightarrow \infty - ib$ .

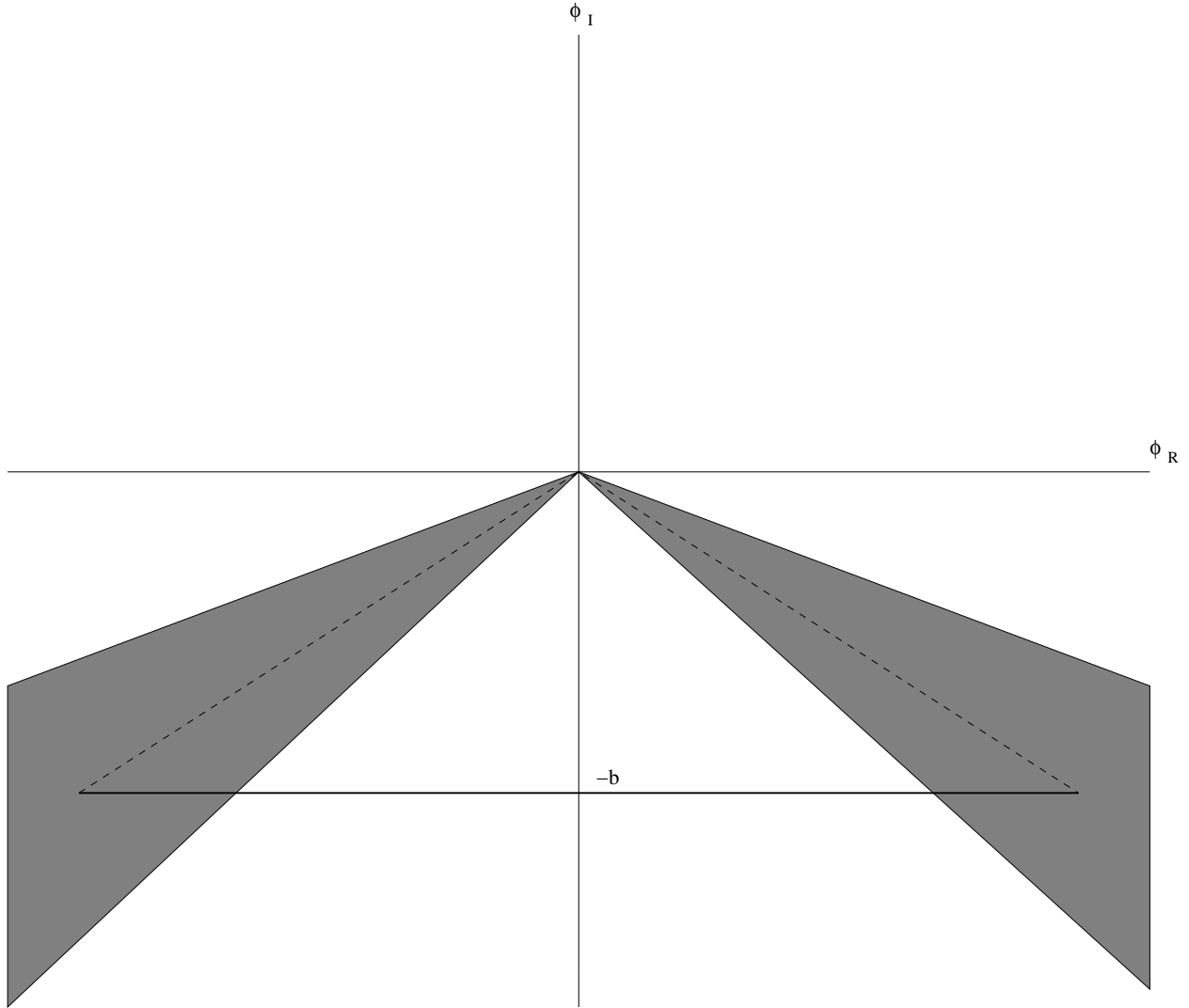


FIG. 2. Typical example of Stokes' wedges for a massless, zero-dimensional  $-g(i\phi)^N/N$  theory. The shaded areas are the regions within which the path integral for a given  $N$  converges because  $\exp(-S(\phi))$  is exponentially damped. The usual path of integration, even for a finite contour, is represented by the dashed line and extends from  $(-b, -b \cot \theta_L)$  to the origin and then from the origin to  $(-b, b \cot \theta_R)$ , where  $\theta_L$  and  $\theta_R$  are given in Eq. 1.2. In order to prove that the Langevin expectation values have the desired behavior as  $\tau \rightarrow \infty$ , it is most convenient to use the smooth contour represented by the solid line. The solid line contour is defined as  $\phi = \phi_R - ib$  and extends from  $(-b, -b \cot \theta_L) \rightarrow (-b, b \cot \theta_R)$ .



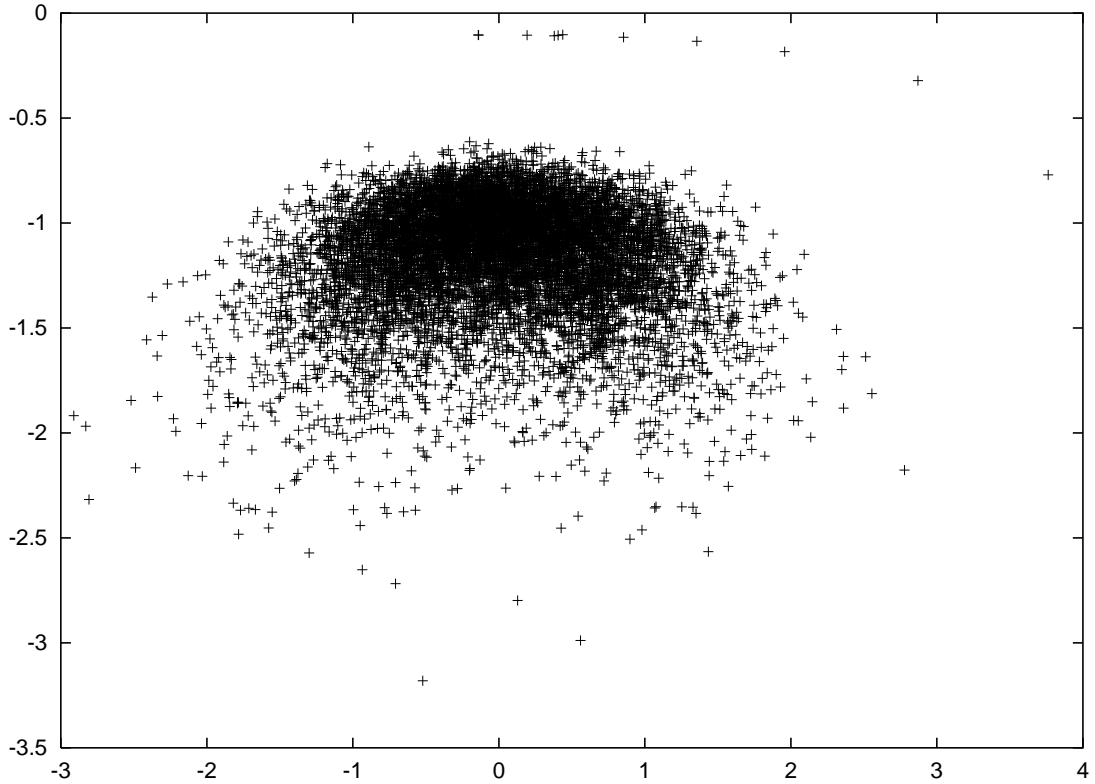


FIG. 3. Plot of the field  $\phi$  in the complex plane for the potential  $-g\phi^4/4$  with  $\epsilon = 0.3$  using the second-order algorithm. Each point corresponds to the value of  $\phi$  for a value of the fictitious time  $\tau$ . The absolute magnitude of  $\phi$  was restricted to be less than 19 in order avoid numerical instabilities. (For simulations of  $-g\phi^4/4$  in one dimension, this restriction was unnecessary.) The first 10,000 points are plotted. The field started at the point  $(0.5, -0.1)$  and then followed a path towards the imaginary axis. It then traveled from side to side forming a cloud of points that averaged to the value  $-1.1687$ .

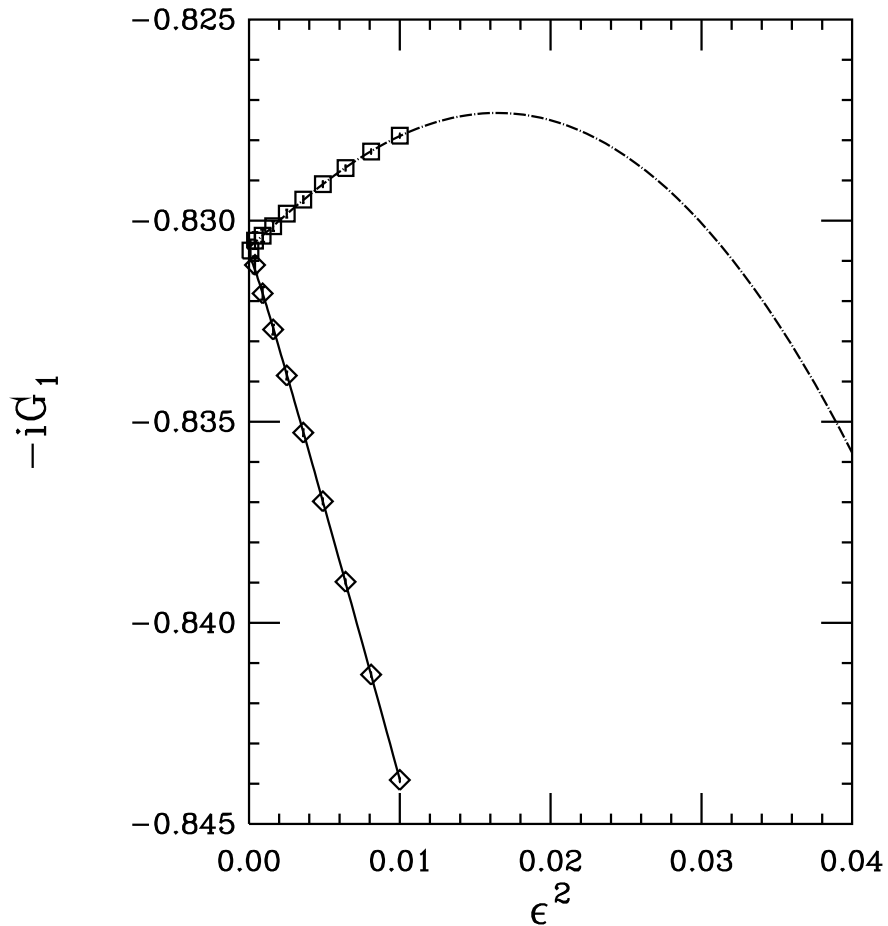


FIG. 4. Plot of values for  $-iG_1$  for a real time spacing of  $a = 0.5$  versus the square of the fictitious time spacing,  $\epsilon^2$ , for a  $-g\phi^4/4$  potential in one dimension. The solid line is a fit that is a linear plus quadratic in  $\epsilon$  for values computed using Euler's method (diamonds). The dashed line is a cubic fit in  $\epsilon$ , without a term that is linear in  $\epsilon$ , for values computed using the second-order algorithm (squares). Similar fits were performed for each value of  $a$  shown in Fig. 5.

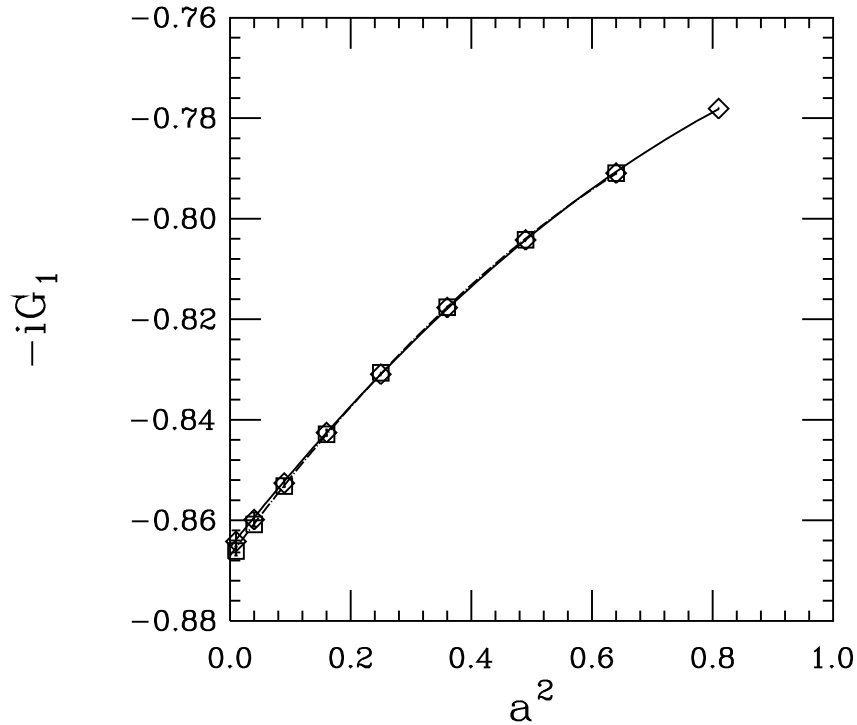


FIG. 5. Extrapolated values of  $-iG_1$  versus real time spacing  $a^2$  for a  $-g\phi^4/4$  potential in one dimension. Lattice expectation values for these theories only depend upon even powers of  $a$ , so fits are done in powers of  $a^2$ . Both fits shown here are linear plus quadratic in  $a^2$ . Diamonds show values computed using Euler's method, and the solid line is a fit for them. Squares show the results from the second-order algorithm; the dashed line is the fit to them. The continuum limit values obtained from these plots are given in Tab. 2. Similar fits were performed for all of the data in Table 2.

## REFERENCES

- [1] C. M. Bender and S. Boettcher, Phys. Rev. Lett. **80**, 5243 (1998).
- [2] C. M. Bender, S. Boettcher, and P. N. Meisinger, J. Math. Phys. **40**, 2201 (1999).
- [3] C. M. Bender and S. Boettcher, J. Phys. A: Math. Gen. **31**, L273 (1998).
- [4] C. M. Bender, G. V. Dunne and P. N. Meisinger, Phys. Lett. A **252**, 272 (1999).
- [5] A. A. Andrianov, M. V. Ioffe, F. Cannata, J.-P. Dedonder, Int. J. Mod. Phys. A **14**, 2675 (1999).
- [6] E. Delabaere and F. Pham, Phys. Lett. A **250**, 25 (1998).
- [7] E. Delabaere and D. T. Trinh, J. Phys. A: Math. Gen. **33**, 8771 (2000).
- [8] M. Znojil, Phys. Lett. A **259**, 220 (1999).
- [9] B. Bagchi and R. Roychoudhury, J. Phys. A: Math. Gen. **33**, L1 (2000).
- [10] F. Cannata, G. Junker, J. Trost, Phys. Lett. A **246**, 219 (1998).
- [11] H. Jones, Phys. Lett. A **262**, 242 (1999).
- [12] G. A. Mezincescu, J. Phys. A: Math. Gen. **33**, 4911 (2000). See also the references therein.
- [13] C. M. Bender and Q. Wang, J. Phys. A: Math. Gen., in press.
- [14] C. M. Bender, F. Cooper, P. N. Meisinger, and V. M. Savage, Phys. Lett. A **259**, 224 (1999).
- [15] K. C. Shin, J. Math. Phys. **41**, 2513 (2001).
- [16] P. Dorey, C. Dunning, and R. Tateo, "Spectral Equivalence from Bethe Ansatz Equations", hep-th/0103051.
- [17] C. M. Bender, K. A. Milton, and V. M. Savage, Phys. Rev. D **62**, 085001 (2000).

- [18] J. R. Klauder, Phys. Rev. A **29**, 2036 (1984).
- [19] J. R. Klauder and W. P. Petersen, J. Stat. Phys. **39**, 53 (1985).
- [20] J. Ambjorn, M. Flensburg, C. Peterson, Nucl. Phys. B **275**, 375 (1986).
- [21] D. Callaway, F. Cooper, J. Klauder, and H. Rose, Nucl. Phys. B **262**, 19 (1985).
- [22] N. Goldenfeld, *Lectures on Phase Transitions and the Renormalization Group*, (Addison-Wesley, Reading, 1998), p. 209.
- [23] C. W. Gardiner, *Handbook of Stochastic Methods*, (Springer-Verlag, Berlin, 1985).
- [24] G. Parisi, Phys. Lett. **131B**, 393 (1983).
- [25] J. Ambjorn and S. K. Yang, Phys. Lett. **165B**, 140 (1985).
- [26] H. Nakazato and Y. Yamanaka, Phys. Rev. D **34**, 492 (1986).
- [27] H. Nakazato, Prog. Theor. Phys. **77**, 20 (1987).
- [28] R. W. Haymaker and Y. Peng, Phys. Rev. D **41**, 1269 (1990).
- [29] S. Lee, Nucl. Phys. B **413**, 827 (1994).
- [30] H. Gausterer, J. Phys. A: Math. Gen. **27**, 1325 (1994).
- [31] C. Adami and S. E. Koonin, Phys. Rev. C **63**, 034319-1 (2001).
- [32] H. Nakazoto, Phys. Rev. D **48**, 5838 (1993).
- [33] G. Parisi and N. Sourlas, Phys. Rev. Lett. **43**, 744 (1979).
- [34] No  $i$ 's must be inserted to insure  $\mathcal{PT}$  symmetry as in Ref. [14].
- [35] E. Helfland, Bell System Tech. J. **58**, 2289 (1979).
- [36] C. M. Bender, S. Boetcher, and V. M. Savage, J. Math. Phys. **41**, 6381 (2000).
- [37] M. Henkel, *Conformal Invariance and Critical Phenomena*, (Springer, Berlin, 1999).

[38] G. Parisi and N. Surlas, Phys. Rev. Lett. **46**, 871 (1981).